MICROSTRUCTURAL ASPECTS OF STRAIN HARDENING AND DYNAMIC STRAIN AGING IN Cu-Zn ALLOYS

A. H. P. de Andrade, Y. Guerin and H. L. Fotedar

PULBICAÇÃO IEA 448 CCTM 33	NOVEMBRO/1978

PUBL. IEA 446
CCTM 33

NOVEMBRO/1976

MICROSTRUCTURAL ASPECTS OF STRAIN HARDENING AND DYNAMIC STRAIN AGING IN Cu-Zn ALLOYS

A. H. P. de Andrade, Y. Guerin and H. L. Foteder

COORDENADORIA DE CIÊNCIA E TECNOLOGIA DE MATERIAIS
(CCTM)

INSTITUTO DE ENERGIA ATÔMICA
SÃO PAULO – BRASIL

APROVADO PARA PUBLICAÇÃO EM MAIO/1976.

INSTITUTO DE ENERGIA ATÔMICA
Caixa Postal 11.049 (Pinheiros)
Cidade Universitária "Armando de Salles Oliveira"
SÃO PAULO – BRASIL

NOTA: Este trabalho foi conferido pelo autor depois de composto e sua redação está conforme o original, sem qualquer correção ou mudança.

MICROSTRUCTURAL ASPECTS OF STRAIN HARDENING AND DYNAMIC STRAIN AGING IN Cu-Zn ALLOYS*

A. H. P. de Andrade, Y. Guerin and H. L. Fotedar**

ABSTRACT

Yielding and work hardening in polycrystalline α-brass are found to be predominantly due to athermal dislocation interactions between the dislocation pile ups produced during straining and the geometrically necessary dislocations generated to maintain compatibility between the grains. Serrated yielding has been explained on the basis of the step-propagation of a deformation band through the gage length.

1 – INTRODUCTION

Dynamic Strain Aging usually refers to process or processes that take place when a material is deformed plastically. Technological importance of this phenomenon lies in its use, to considerably increase the strength of b.c.c. metals and alloys, in conjuction with cyclic prestraining[19]. Strengthening methods based on this process are called multiple-mechanical thermal treatments[15].

In recent years dynamic strain aging has been extensively studied in interstitial and substitutional b.c.c.[2,7-8,11,18,20-22,25] and f.c.c.[3-5,10,13-14,16,23-24] alloys, as well as in a number of ionic solids[6,9,17]. This type of deformation usually manifests itself in the form of serrated stress strain curve over a specific range of temperature and strain rate and a uniform deformation a critical strain ϵ_c, which is temperature and strain rate dependent, normally preceeds the serrations in the stress-strain curves.

The serrated yielding has been explained by Cottrell[7] as due to the strain enhanced diffusion of substitutional solutes to form atmospheres at dislocations. The attendant attempts of dislocations to alternately break away or be pinned by these atmospheres leads to serrations in the load-elongation curves. In the case of substitutional alloy systems[8,12], however, considerable controversy exists about the general applicability of Cottrell's model. Recently Cuddy and Leslie[8] have proposed that serrations can also arise from the formation and propagation of bands of localized deformation when using a hard testing machine. Furthermore to date no datailed study is avialable which takes into account the influence of a dispersed second phase on the dynamic strain aging characteristics of a duplex alloy.

In the present work preliminary results of microstructural aspects of serrated yielding and work hardening in α and $(\alpha + \beta)$ brass are reported, as a function of temperature and deformation rate.

2 – EXPERIMENTAL METHOD

Two commercial brass sheets containing 30 and 36% Zn respectively were purchased from Impormetal-Betina S.A., São Paulo, Brazil. Tensile specimen 3 cm gage length, 6 mm width and 0,6 mm thickness were machined from the sheets. Machined Cu – 30% Zn test specimen were annealed at 450°C for 1 hour in Argon to give a single phase microstructure with a mean α-grain size of about 100 μ. The

---

(*) Presented at the IV Interamerican Conference on Materials Technology June 29 - July 4, 1975, Caracas - Venezuela.
(**) Will present the paper.

Cu – 36% Zn test specimen were subjected to a series of heat treatments in salt baths followed by water quenching to obtain duplex ($\alpha+\beta$) microstructure with various volume fractions of β-phase.

The specimens were electropolished and deformed in an Instron Universal testing machine equipped with push button rate change controls, stepwise load supression and a furnace capable of using either Argon or vacuum atmosphere. Tests were conducted in air at the deformation rate of 1.7×10^{-1} to 1.7×10^{-3}/min, in the temperature range of 24-150°C.

The deformed specimen were first examined in optical microscope & then electrolytically thinned to produce a thin foils by window technique, using the following conditions.

Electrolyte	40% H_3PO_4, 60% water
Cathode	stainless steel
Temp	0°C
Voltage	1.6 to 2.0 v
time	15 min

The thin specimen were then examined in either 60 KV Zeiss or 100 KV Elmiskop I transmission electron microscopes.

3 – RESULTS

3.1 – Stress-strain Characteristics:

Figure 1 shows characteristics true stress-true strain curves of polycrystalline α-brass as a function of strain rate at room temperature. Main data deduced from this curve are given in table I. In table II are gathered data obtained at different temperatures and constant strain rate. The yield stress, work hardening rates and fracture strain of α-brass are not significantly affected by variation of temperature or strain rate. The flow stress at room temperature exhibits a slight reverse strain rate dependence which is typical of dynamic strain aging[25]. At room temperature the work hardening rate of ($\alpha+\beta$) brass is about 40% higher than that in α brass.

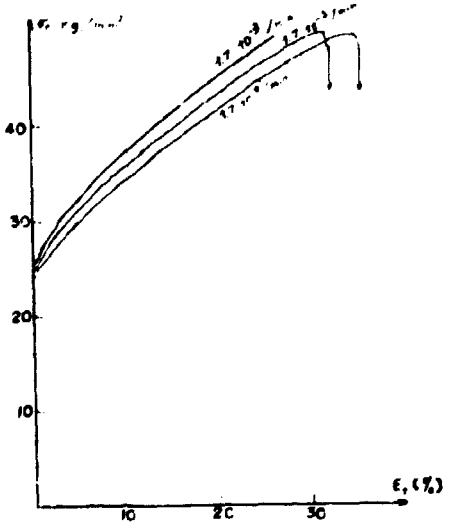

Figure 1 – True Stress True Plastic Strain Curves of α Brass as a Function of Strain Rate at Room Temperature

Table I

Comparison of yield stress (0.2% offset), fracture strain and work hardening rates ($\theta = d\sigma/d\epsilon_p$) at different strains as a function of strain rate at room temperature in α brass (Cu – 30% Zn)

Strain Rate (min^{-1})	Yield Stress (Kg/mm^2)	Fracture Strain (%)	Work Hardening Rate (θ) (Kg/mm^2)		
			$\epsilon = 5\%$	$\epsilon = 10\%$	$\epsilon = 20\%$
1.7×10^{-1}	23.9	42.6	93	76	54
1.7×10^{-2}	25.4	38.5	96	78	70
1.7×10^{-3}	25.9	–	105	85	71

Table II

Comparison of yield stress (0,2% offset) fracture strain and work hardening rates ($\theta = d\sigma/d\epsilon_p$) at different strains as a function of temperature at a strain rate of 1.7×10^{-2}min in α-brass (Cu – 30% Zn)

Temp. (°C)	Yield Stress (Kg/mm^2)	Fracture Strain (%)	θ (Kg/mm^2)		
			$\epsilon = 5\%$	$\epsilon = 10\%$	$\epsilon = 20\%$
24	25.4	38.5	96	78	70
100	25.4	33.5	99	83	70
150	24.7	41.7	85	73	62

3.2 - Dynamic Strain Aging

All the tests on α and (α + β) brasses at 24°C, 100°C and 150°C exhibit serrated stress-strain curves, with no detectable critical strain, except at room temperature and high strain rates ($1,7 \times 10^{-1}$ /min).

Figure 2 shows the effect of temperature and second phase (β) on the serrated yielding characteristics of Cu-Zn alloys. In α brass at room temperature and strain rate of 1.7×10^{-2} /min, irregular jerky flow is observed from the beginning of yielding as shown in figure 2a. The amplitude of the most important serration is of the order of 0.3 Kg/mm^2. At lower strain rates ($1,7 \times 10^{-3}$ /min) the serrations become more regular after some pre-deformation. The mean amplitude of the serration is about 0.15 Kg/mm^2.

At 100°C and 150°C the stress-strain curves for α -brass exhibit regular Russel type B' serrations[23] producing rapid fluctuations of flow stress (figure 2b). The amplitude of the serrations is about 0.3 Kg/mm^2 and the period corresponds to a deformation of 0.01%. At large strains, however, the amplitude decreases to the order of 0.1 Kg/mm^2 and the serration take increasingly irregular character with the intermitant occurance of large yield drops of about 0.5 Kg/mm^2.

Figure 2c shows serrated stress-strain characteristics of an $(\alpha + \beta)$ brass at 24°C. The presence of β-phase seems to lower the amplitude of serrations of almost regular character to about 0.1 Kg/mm^2.

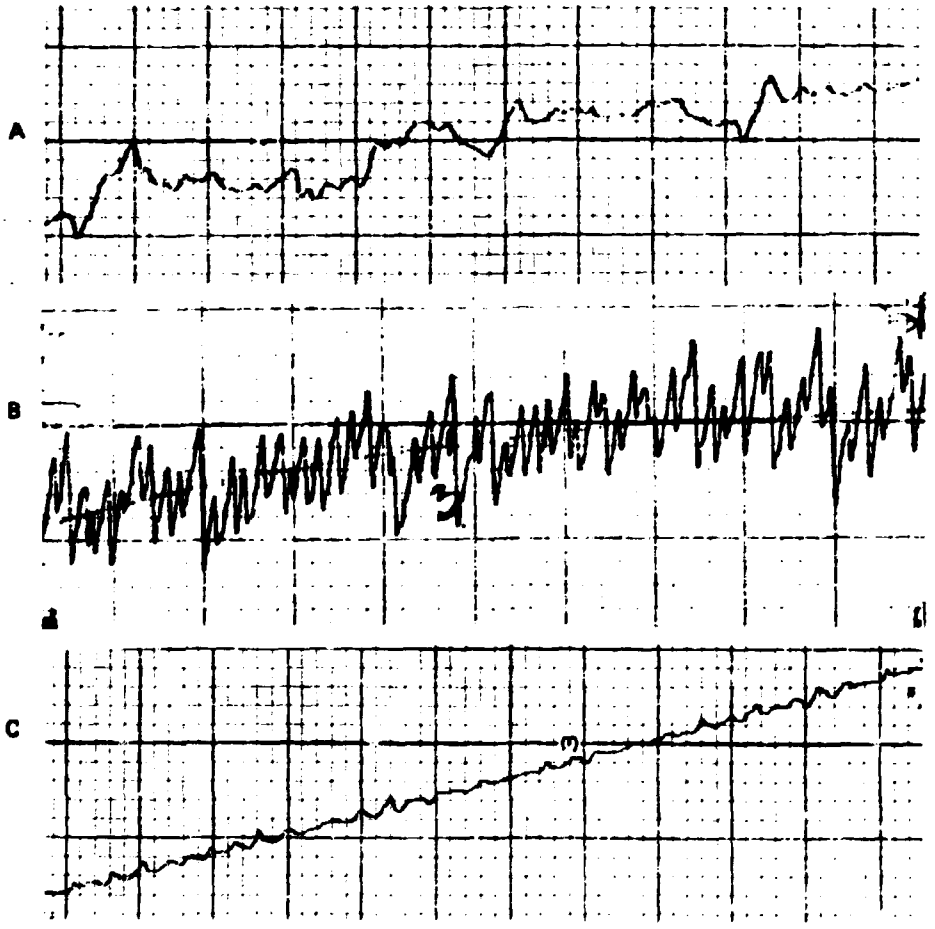

Figure 2 — Traces of Instron Chart Recordings of the Stress-Strain Curves Registered at a Strain Rate of 1.7×10^{-2}/min
a) on α brass at room temperature
b) on α brass at 100°C
c) on $(\alpha + \beta)$ brass at room temperature. One small vertical division corresponds to a stress of 0,1 Kg/mm^2 and one small horizontal division is 0,014% strain

3.3 — Microstructure

Figure 3 shows an optical micrograph of a fractured polycrystalline α-brass at room temperature. A large number of slip lines are piled up on grain boundaries. In general slip lines belonging to the two most favoured slip systems of the type (111) <110> appear in each grain. In addition some wavy slip lines are also observed in some heavily deformed grains.

Figure 4 shows an optical micrograph of an $(\alpha + \beta)$ brass tensile tested at 150°C. Most of the α-grains are heavily deformed with the activation of at least three slip systems. Slip lines are not visible in the β phase because of the very high speed of the attack in that phase. An important microscopic observation is that slip lines of the same orientation can be seen in some α-grains seperated by a β-phase.

Figure 3 – Optical Micrograph of an α Brass Sample Deformed Up to Fracture at Room Temperature (X200)

Figure 4 – Optical Micrograph of an (α + β) Brass Sample Deformed Up to Fracture at 150°C (X200)

Figure 5 shows the transmission electron micrograph of an α-brass specimen deformed to fracture at room temperature and a deformation rate of 1.7×10^{-1} /min.

The deformed microstructure consists of characteristic planer arrangements of partial dislocations in pile up formation. These pile ups are indicated by arrows.

Figure 6 shows the transmission electron micrograph of an as received α-brass showing a higher dislocation density. Again arrangements of partial dislocation are seen in pile up formation, along with a group of straight dislocations trying to glide through these pile ups.

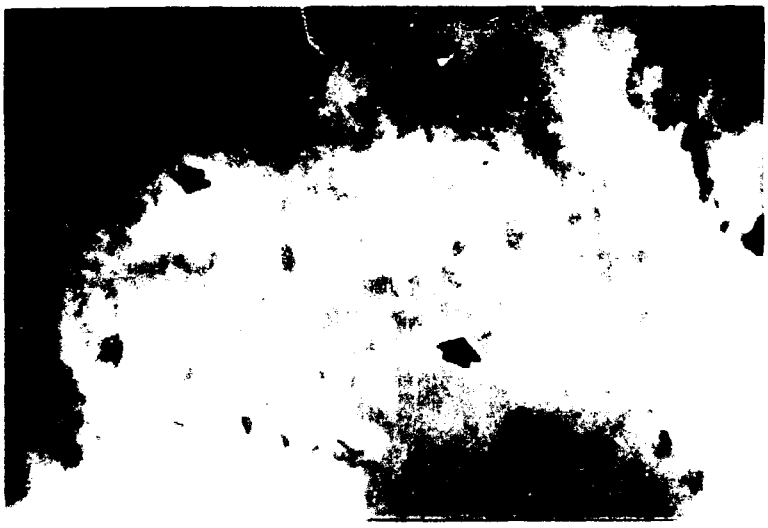

Figure 5 – Transmission Electron Micrograph of α Brass Deformed to Fracture at Room Temperature and a Strain Rate of 1,7 X 10^{-1}/min (X200,000).

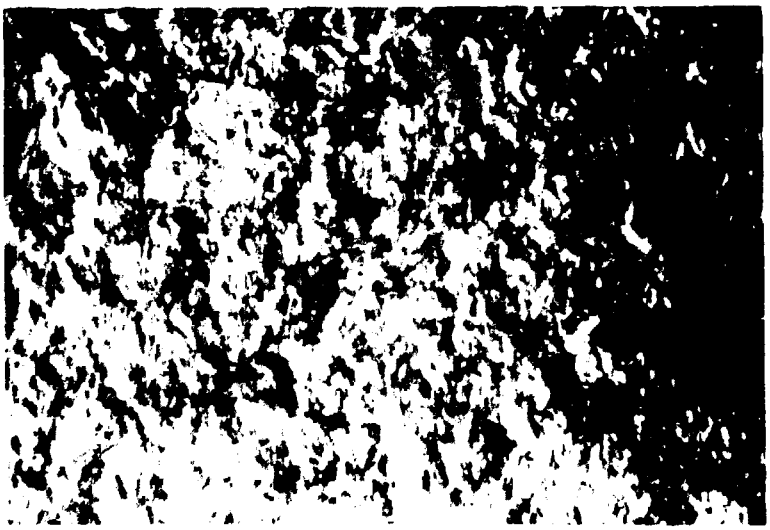

Figure 6 – Transmission Electron Micrograph of an As Received α Brass (X84,000)

4 – DISCUSSION

The deformation process in polycrystalline α-brass commences by the slip of fresh dislocations in some isotropic grains having most favorably oriented slip systems, with maximum resolved shear stress. As the deformation proceeds these dislocations will pile up against obstacles such as grain boundaries. According to Ashby[1] secondary dislocations also called "geometrically necessary dislocations" must be generated at the grain boundaries to maintain the compatibility between the grains during deformation. The back stress of the pile ups on the Frank-Read sources and the long range interaction with the geometrically stored dislocations are the two main internal stresses the moving dislocations must overcome in the early stages of deformation, both of these give rise to essentially long-range athermal stresses which explains why the yield stresses observed in α-brass are temperature and strain rate independent, as shown in Table I and II.

Recently Korbel[12] has pointed out some of the limitations of Cottrell's model in describing the dynamic strain aging in α-brass. Therefore it is only appropriate to explain the jerky flow in terms of step propagation of a deformation band as suggested by Cuddy and Leslie[8].

The high local stresses at the head of a dislocation pile up near the grain boundary can activate new slip bands in the adjacent grains and the deformation proceeds by the propagation of these bands. The irregular serrations in α-brass at room temperature (figure 2a) can be attributed to the localized rapid movement of these deformation bands causing bursts of strain resulting in load drops in a hard testing machine. Immediately after the formation of a new band the applied stress is too low to move this deformation band, hence stress increases elastically to a level sufficient to reinitiate the propagation of the band front. The serrations between the two main load drops corresponds to the propagation of one band over the entire or part of the gage length and therefore depicts a spectrum of the internal stresses the deformation band has to overcome as it moves along the gage length.

At high temperature or low strain rate, aging of the dislocations at the band front dislocations occurs during the reloading time. Thereafter, a higher stress is needed to either unpin them or nucleate fresh dislocations and the process repeats, leading to regular Russel "B" type serrations (figure 2b). Up to now, we are not able to say what exactly causes the aging: it cannot be the condensation of solute zinc atoms, because, as said above, these atoms are always forming fairly condensed atmosphere near every dislocation, it can hardly be condensation of low concentration impurities atoms because this would require a initial uniform deformation, it is more likely a rearrangement of the solute in the vicinity of the dislocation, some short range order or some type of reorientation of solute impurity complexes.

The aging effect is stronger at higher temperature causing a higher magnitude of the serrations. The slightly reverse strain rate dependance of the work hardening of α-brass at room temperature (see Table II) is probably due to the same reason: at lower strain rate, pinning is more effective, so that higher stresses are needed to pull the dislocations, also probability to nucleate fresh ones is higher and the resulting increasing in the dislocation density causes an increased work hardening rate.

In $(\alpha + \beta)$ brass the presence of the harder β phase is likely to make the relaxation of pile ups more difficult and a greater number of geometrically necessary dislocations is probably generated; consequently a higher number of slip systems is activated so that the work hardening rate is greater. But the β phase is not an insurmontable barrier; as it is seen in figure 4, slip lines of the same orientation can be encountered in two grains separated by β phase (the two α grains are probably part of the same α grain from which β phase precipitated). The serration yielding is probably due, as in α brass, to the step propagation of a deformation band through the α and β phase. The high density of the geometrically necessary dislocations interacting with the pile ups may be responsible for the lower magnitude of the serrations.

ACKNOWLEDGMENTS

We wish to thank Dr. I. Falleiros for providing experimental facilities in the Department of Metallurgical Engineering of the Escola Politécnica, U.S.P., and Dr. H. S. Santos of the Centre for Electron Microscopy U.S.P., for the use of 100 KV Elmiskop I electron microscope.

RESUMO

Encontrou-se que o escoamento e o encruamento do latão α policristalino são devidos predominantemente a interações atérmicas das discordâncias, entre os empilhamentos de discordâncias produzidos durante a deformação e as discordâncias necessárias geometricamente geradas para manter a compatibilidade entre os grãos. O escoamento serrilhado foi explicado com base na propagação por etapas de uma banda de deformação através do comprimento útil do corpo de prova.

REFERENCES

1. ASHBY, M. F. The deformation of plastically non-homogeneous materials. *Phil. Mag.*, London, 21:399-424, 1970.

2. BERGSTROM, Y. & ROBERTS, W. The application of a dislocation model to dynamical strain ageing in α-iron containing interstitial atoms. *Acta metall.*, Toronto, 19:815-23, 1971.

3. BONISZEWSKI, T. & SMITH, G. C. The influence of hydrogen on the plastic deformation ductility and fracture of nickel in tension. *Acta metall.*, Toronto, 11:165-78, 1963.

4. BRINDLEY, B. J. & WORTHINGTON, P. J. Serrated yielding in aluminium-3% magnesium. *Acta metall.*, Toronto, 17:1357-61, 1969.

5. _____ & WORTHINGTON, P. J. Yield-point phenomena in substitutional alloys. *Metall. Rev.*, London, (45):101-14, 1970.

6. BROWN, L. M. & PRATT, P. L. Strain ageing in $CdCl_2$-doped rock salt. *Phil. Mag.*, London, 8:717-34, 1963.

7. COTTRELL, A. H. A note on the Portevin-Le Chatelier effect. *Phil. Mag.*, London, Ser. 7, 44:829-32, 1953.

8. CUDDY, L. J. & LESLIE, W. C. Some aspects of serrated yielding in substitutional solid solutions of iron. *Acta metall.*, Toronto, 20:1157-67, 1972.

9. FOTEDAR, H. L. & STOEBE, T. G. Dynamic strain ageing in LiF single crystals. *J. Phys.*, Paris, 34:C9/367-C9/71, 1973.

10. JENKINS, C. F. & SMITH, G. V. Serrated plastic flow in austenitic stainless steel. *Trans. metall. Soc. A.I.M.E.*, New York, 245:2149-56, 1969.

11. KEH, A. S. et alii. Dynamic strain aging in iron and steel. In: ROSENFIELD, A. R. et alii, eds. *Dislocation dynamics*. New York, McGraw-Hill, 1968. p.381-408.

12. KORBEL, A. The structural aspects of the Portevin-Le Chatelier effect in alpha brass. *Scr. metall.*, Long Island City, N. Y., 8:609-12, 1974.

13. LUBAHN, J. D. Simultaneous aging and deformation in metals. *Trans. Am. Inst. Min. Metall. Engr, Metals Trans.*, New York, 185:702-7, 1949.

14. McCORMICK, P. G. Effect of grain size on serrated yielding in an Al-Mg-Si alloy. *Phil. Mag.*, London, 23:949-56, 1971.

15. McELROY, R. J. & SZKOPIAK, Z. C. Dislocation-substructure-strengthening and mechanical-thermal treatment of metals. *Int. metall. Rev.*, London, 17:175-202, 1972.

16. McREYNOLDS, A. W. Plastic deformation waves in aluminum. *Trans Am. Inst. Min. Metall. Engr, Metals Trans.*, New York, 185:702-7, 1949.

17. MOON, R. L. & PRATT, P. L. *Proc. Br. Ceram. Soc.*, Stoke-on-Trent, Engl., 15:203, 1970.

18. NAKADA, Y. & KEH, A. S. Kinetics of snoek ordering and Cottrel atmosphere formation in Fe-N single crystals. *Acta metall.*, Toronto, 15:879-83, 1967.

19. ODING, I. A. et alii. Effects of repetead creep with intermediate aging on the strength of body-centered cubic metals. *Soviet Phys. Dokl.*, New York, 10:75-7, 1965.

20. PINK, E. Conditions for serrated yielding in Va and VIa-group metals. *Trans. metall. Soc. A.I.M.E.*, New York, 245:2597-8, 1972.

21. PORTEVIN, A. & LE CHATELIER, F. C. R. Sur une phénomène observé lors de l'essai de traction alliages en cours de transformation. *C. r. hebd. Séanc. Acad. Sci.*, Paris, 176:507-10, 1923.

22. RAFFO, P. L. Dynamic strain aging during the creep of a Mo-Ti-C alloy. *Trans. Am. Soc. Metals*, Chicago, 62:846-51, 1969.

23. RUSSEL, B. Repetead yielding in tin bronze alloys. *Phil. Mag.*, London, 8:615-30, 1963.

24. SONON, D. E. & SMITH, G. Effect of grain size and temperature on the strengthening of nickel and a nickel-cobalt alloy. *Trans. Metall. Soc. A.I.M.E.*, New York, 242:1527-33, 1968.

25. YOSHINAGA, H. et alii. The Portevin-Le Chatelier effect in vanadium. *Phil. Mag.*, London, 23:1387-403, 1971.